



www.editada.org

## Comparative Study of Lung Image Representations for Automated Pneumonia Recognition

Angel Ernesto Picazo Castillo<sup>2</sup>, Salvador E. Ayala Raggi<sup>1</sup>, Leopoldo Altamirano Robles<sup>2</sup>, Aldrin Barreto Flores<sup>1</sup>, José Francisco Portillo Robledo<sup>1</sup>

<sup>1</sup> Benemérita Universidad Autónoma de Puebla, Puebla, México.

<sup>2</sup> Instituto Nacional de Astrofísica, Óptica y Electrónica, Puebla, México.

angel.picazo@inaoep.com, saraggi@gmail.com, robles@inaoep.mx

**Abstract.** This paper presents a method for automatic pneumonia recognition by localizing and normalizing the position, rotation, and scale of lung regions in chest X-ray images. Likewise, we propose a classifier composed by: "Eigenfaces" method for feature reduction, Fisher's discriminant criterion for feature selection, and a Multilayer Perceptron (MLP). We showed that a proper lung region alignment improves accuracy in several classifiers. Several CNN classifiers (MobileNetV2, ResNet-50, ResNet-18, Compact, and AlexNet), and our feature-discrimination-based classifier were tested with non-aligned images from a semantic segmentation stage, and on the other hand, with aligned images from our proposed normalization stage. Results show that the proposed normalization method improves MobileNetV2's accuracy to 97.1%, compared to 95.3% when using semantic segmentation. Furthermore, our proposed classifier based on feature discrimination increases its accuracy to 97.3% when using the normalization stage. Our classifier and normalization method achieve comparable or superior results to CNN classifiers.

**Keywords:** Pneumonia, CNNs, Image segmentation, MLP, Image Classification, Fisher's Ratio.

Article Info

Received May 10, 2024.

Accepted Nov 24, 2024.

## 1 Introduction

Pneumonia is a respiratory condition caused by bacteria and viruses, with infection possible through airborne particles, saliva, or mucus. Notably, children and older adults are more susceptible to this ailment, as reported by (World Health Organization, 2016). Consequently, Chest X-rays (CXRs) have emerged as a prevalent and cost-effective diagnostic method, as seen in (Alzaharani et al., 2017; Amatya et al., 2018; Moberg et al., 2016). Despite the widespread availability of Chest X-ray (CXR) machines, their utility for rapid and comprehensive screening is hindered by challenges faced by radiologists in interpreting ambiguous radiological features, such as consolidation and hazy increased opacities, as observed in (Niedermaier & Torres, 2022; Ticinesi et al., 2016). Integrating AI-driven systems into medical diagnosis has exhibited significant advancements in supporting radiologists and clinicians in disease detection, characterization, and monitoring. However, the current challenge lies in the lack of uniformity in the alignment and brightness of the region of interest (the lungs) in labeled radiographs available in information repositories, as illustrated in (Chowdhury et al., 2020; Rahman et al., 2021). The establishment of these repositories has been a collaborative effort involving institutions and medical experts in the field, as mentioned in works such as (Ghaderzadeh et al., 2021; Qin et al., 2018; Salvatore et al., 2021). Some of these radiographs contain undesired or irrelevant information for classification,

potentially impacting the accuracy metrics of machine learning algorithms, as discussed in (Budimirovic et al., 2022; Rahman et al., 2021).

Additionally, the contrast enhancement in radiographs is crucial as it facilitates the detection and diagnosis of pathologies. Improved contrast allows for clearer differentiation of various body structures and tissues, highlighting anomalies and fine details that could indicate diseases. Moreover, good contrast can reduce the need for additional tests and minimize diagnostic errors, thereby improving precision and efficiency in medical care (Lee et al., 2023).

In this study, a comparison is conducted between two image preprocessing methods, along with the application of the contrast enhancement method Contrast Limited Adaptive Histogram Equalization (CLAHE), applied to both training and test images for subsequent classification. The first method involves semantic segmentation of the region of interest to extract images containing only the lungs, as described in (Rahman et al., 2021). The second method is a proposed approach aiming to align the region of interest so that anatomical structures within the lungs match in position across all images. Notably, this image normalization process is carried out without using deep learning algorithms. CLAHE has proven to be effective, showing good results in radiographs. Therefore, this method will be applied to the images used in the experiments. The objective of the comparison is to determine which representation of the radiographs (semantic segmentation or normalization) achieves a higher classification accuracy. Additionally, the study aims to observe whether CLAHE can further improve classification results.

For image classification, various convolutional neural networks (CNNs) such as MobileNetV2, ResNet-50, ResNet-18, Compact, and AlexNet are employed, all of which are available in the MVTEC Deep Learning Tool program. A proposed classifier is introduced, initially using the “Eigenfaces” method for dimensionality reduction of radiographic images, a technique based on Principal Component Analysis (PCA). Next, the selection and weighting of the most discriminative features are performed using the Fisher discriminant criterion (FDR). Finally, a Multi-Layer Perceptron (MLP) algorithm is used for classification. The objective here is to compare a classifier algorithm that does not use a convolution-based image methodology and to determine if it can achieve accuracy rates comparable to those of CNNs.

As a result, a two-step sequential process is proposed in our classifier. The first step involves image preprocessing, encompassing lung region detection and normalization. In other words, the goal is to ensure that images within the lung region have the same alignment, location, and scale as much as possible, along with contrast enhancement using CLAHE, which has proven effective in radiographs. The second process aims to optimize features by implementing the “Eigenfaces” (PCA) on the aligned images. This results in obtaining a condensed set of statistically independent features. Finally, based on the Fisher discriminant criterion described in (Silva, 2019a), it is recommended to perform a selection of features that achieve enhanced discrimination between classes. Utilizing this set of optimized features and a conventional classifier like the MLP, the objective is to achieve classification accuracy values comparable to those obtained through CNNs.

This work is organized into six sections. Section 2 provides a comprehensive analysis of the state-of-the-art related to the central theme of this research, namely image preprocessing and feature selection. Section 3 presents the theory and results of our proposed algorithm, named “The Lung Finder Algorithm” (LFA), which plays a crucial role in the normalization process. Section 4 details the dataset used in this study, including its composition and characteristics. Additionally, the experiments to be conducted are defined, setting the stage for presenting results and discussions in Section 5. Finally, Section 6 summarizes the conclusions derived from this work and suggests potential approaches for future research.

## 2 Related Work

Various studies have been developed to classify chest X-ray images diagnosed with pneumonia, as seen in (Chowdhury et al., 2020; Gazda et al., 2021; Hamza et al., 2022; Khan et al., 2023; Nillmani et al., 2022; Rahman et al., 2021). These works employ deep learning algorithms, such as convolutional neural networks, differing in the proposed network models and image preprocessing techniques. Kundur et al. utilized VGG16, ResNet, InceptionNet, DenseNet models, and a custom CNN model without employing image preprocessing, achieving a classification accuracy of 87.5%. Kavitha et al. also did not use image preprocessing in their CNN model and achieved an accuracy of 89%. On the other hand, Ramli et al., 2023 employed Discrete Wavelet

Transform (DWT) and a bilateral filter for image preprocessing, achieving a model accuracy of 96%. Mydhili et al. used preprocessing methods such as resizing images to a consistent size and normalizing pixel values, resulting in a 97% accuracy. In summary, proper image preprocessing is crucial for achieving higher classification accuracy.

Additionally, some works do not use CNN models in their classification and still achieve high accuracy percentages, as in (Budimirovic et al., 2022; Mohammed et al., 2021). These studies share the methodology of image preprocessing and feature enhancement. Mohammed et al. employed a Gaussian filter and contrast enhancement as preprocessing steps, with Local Binary Pattern as feature extraction, achieving a 94.7% accuracy. Budimirovic et al. used a Median Filter as preprocessing and a Histogram of Oriented Gradients as feature extraction, achieving an impressive 97% accuracy. It can be observed that proper preprocessing and feature extraction techniques significantly enhance classification accuracy results for any algorithm. Table 1 compares related works, including their respective image preprocessing techniques, feature extraction methods, classifier algorithms, and classification accuracy percentages from (Baltazar et al., 2021; Budimirovic et al., 2022; Kavitha et al., 2023; Kundur et al., 2023; Mohammed et al., 2021; Mydhili et al., 2023; Ramli et al., 2023).

**Table 1.** Chest X-ray Classification Studies

Authors	Image Preprocessing	Feature Extraction	Classifier	Accuracy
Kundur et al. (2023)	Not used	Not used	VGG16, ResNet, Custom CNN	87.5%
Kavitha et al. (2023)	Not used	Not used	Custom CNN	89%
Ramli et al. (2023)	DWT, bilateral filter	Not used	Custom CNN	96%
Mydhili et al.(2023)	Image resize and pixel normalization	Not used	Custom CNN	97%
Baltazar et al.,(2021)	Dilation and erosión, HE	Minimum redundancy algorithm	AlexNet, VGG-16	96.84%
Mohammed et al., (2021)	Gaussian Filter, AHE	Local Binary Pattern	SVM	94.6%
Budimirovic et al.,(2022)	Median Filter, HE	Histogram of Oriented Gradients	SVM	97%

### 3 The Lung Finder Algorithm (LFA)

The objective of this algorithm is to locate the lungs in chest radiographs, and it consists of a training and testing stage, as illustrated in Figure 1. During the training phase, 400 images were randomly selected from the Pneumonia, COVID-19, and Normal classes dataset. Histogram equalization (HE) was applied to all images, and the regions of interest were manually labeled by placing four provisional reference points, which are easily locatable by a human user. It was agreed that two of these points would be positioned at the center of the cervical vertebrae, just at the upper boundary of the lungs. The second point was placed on the spine but below the lung region. The last two provisional points required the user to place them along an imaginary straight line perpendicular to the spine, intersecting it right in the middle of the two previous reference points. These last two points were positioned on the left and right sides of the lung region. Finally, four definitive and permanent reference points were calculated at the corners of the rectangular lung region using these four provisional positions.

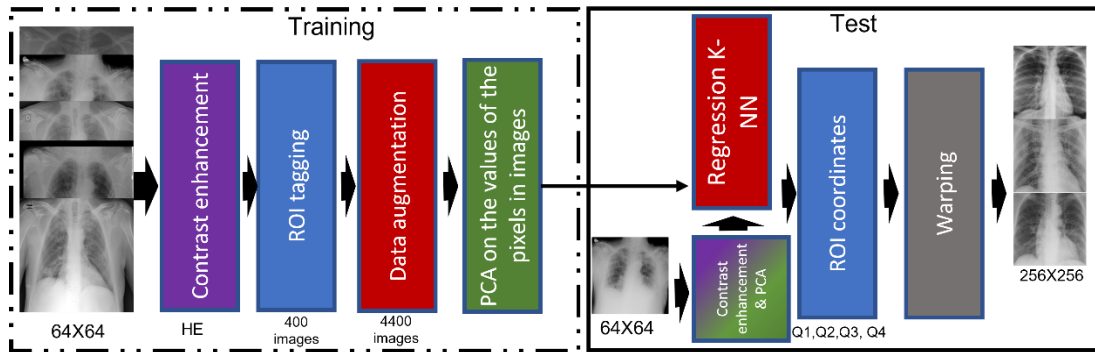


Figure 1. Description of the Lung Finder Algorithm (LFA). At the entrance of the testing stage, a new example is presented, and at the output, the Region of Interest (ROI) is automatically extracted.

Data augmentation was employed with a rotation range of  $-10^\circ$  to  $10^\circ$ , following the recommendation in (Rahman et al., 2021), while for translation, a range of  $-5$  to  $5$  pixels was considered. These ranges ensured that the points of the Region of Interest (ROI) maintained a normalized distribution. Subsequently, a dimensionality reduction technique known as “Eigenfaces,” based on Principal Component Analysis (PCA), as proposed in (Kirby & Sirovich, 1990; M. Turk & Pentland, 1991), was applied. This procedure was performed on the set of 4400 generated images, allowing the creation of a linear subspace capturing the most significant variations in the data. During the testing phase, after contrast enhancement through histogram equalization (HE), each new image was projected into the “Eigenfaces” linear subspace. This transformation converted the image into a compact vector of reduced dimensions. Then, using Euclidean distance, this vector was compared to each of the 4400 examples in the augmented dataset, identifying the  $k$  nearest neighbors through the Weighted  $k$ -NN algorithm. The reference points associated with these  $k$  most similar images from the augmented dataset were used to predict the four reference points of the test image through interpolation. These predicted points represent the coordinates of the corners of the lung ROI. These coordinates enable the warping operation of the interior region of the image towards a standard template of fixed size,  $256 \times 256$  pixels, facilitating consistent extraction of the ROI. Figure 2 presents cases of the warping operation and ROI extraction to exemplify this process. This algorithm has already been tested in the article Ayala-Raggi et al., 2023 and is available for download at: <https://github.com/picazo07/LFA>. For a more comprehensive and detailed explanation of the LFA, we encourage readers to visit the link and review the article.

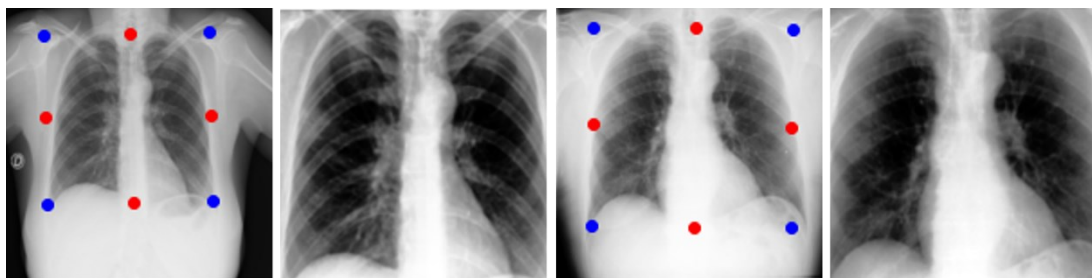


Figure 2. Example images with their extracted regions of interest in normalized images. The red coordinates are obtained through regression, while the blue ones are used to warp the ROI.

### 3.1 Features Reduction

After applying the Lung Finder Algorithm (LFA) to all the radiographs in the dataset to extract the regions of interest, these new images undergo additional preprocessing before being subjected to classification. For our proposed Classifier, we use the “Eigenfaces” as a feature reduction method, based in (Kirby & Sirovich, 1990; M. A. Turk & Pentland, 1991). Additionally, we incorporate the statistical analysis of these features using Fisher’s linear discriminant, seen in (Silva, 2019). The combination of these two methods ensures obtaining a reduced number of features that better discriminate between classes for subsequent classification. The “Eigenfaces” method is based on Principal Component Analysis (PCA) and aims to reduce the dimensionality of images in the database. As each pixel becomes a dimension or variable to analyze, processing high-resolution

images, such as those of 256x256, can be computationally intensive. Each “Eigenface” image displays a structure of common features or patterns in the used image set. These “Eigenfaces” are sorted by the variance of the input images and can be used to reconstruct any image as a linear combination of them, allowing representation in a lower-dimensional space. Figure 3 presents the equation of “Eigenfaces” and the matrix Q of “Eigenfaces.” However, input images must have similar lighting and angle conditions. For this reason, the LFA is used beforehand as a method to normalize radiographs.

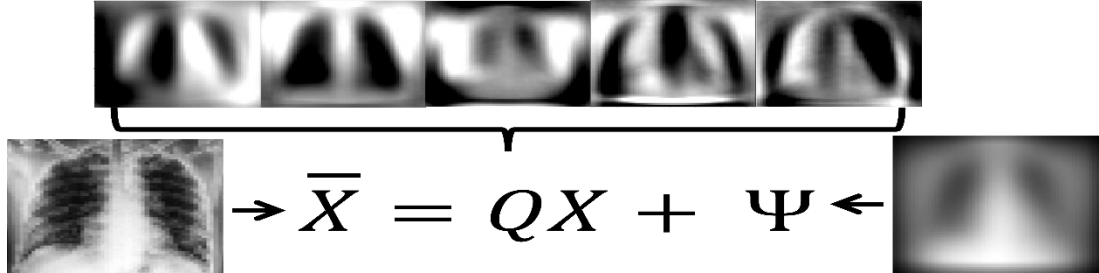


Figure 3. Output image (Left) as the linear combination of the Eigenfaces matrix Q (Center) and the input image plus the mean face (Right).

### 3.2 Feature Selection and Weighting Through Fisher’s Discriminant

The Fisher Discriminant Criterion, also known as the Fisher Ratio (FR), is used in Linear Discriminant Analysis to find a linear projection of features that maximizes class separation. Typically, in two-class problems, only one crucial feature survives this process. However, since the features obtained through PCA are statistically independent to some extent, we can use the Fisher Ratio as a measure of separation between classes for each feature. This process involves evaluating each feature individually, ensuring that the means of observations in each class are as separated as possible while the variances within each class are as small as possible (Silva, 2019). Using this analysis, it is possible to select multiple features obtained through the Eigenfaces method that best discriminate between classes in the dataset. The formula for the Fisher Ratio is found in Equation 1, and the obtained value is denoted as J. It is possible to use the FR to rank the PCA-derived features in descending order according to their discriminative power. This allows for the creation of an array formed by the selected features.

$$J_i = \frac{(\mu_{ic0} - \mu_{ic1})^2}{\sigma_{ic1}^2 + \sigma_{ic2}^2} \quad (1)$$

We propose using the value of the Fisher Ratio (FR) J as a weight for each feature, so that features with higher discriminatory capacity are amplified. We call this methodology “**feature weighting**”. As a first step, we standardize all selected features to give them uniform relevance. Then, we calculate  $\rho_k = \sqrt{J_k}$  for each feature k. Next, we normalize  $\rho_k$ , as shown in Equation 2. Finally, each  $\rho_k$  is used to weigh its respective feature k. The goal is to assign greater importance in classification to features with higher discriminative power.

$$\rho_k = \frac{\rho_k}{\sum_{i=1}^k \rho_i} \quad (2)$$

In the figure 4, the transformation of the data through our methodology used by our proposed classifier can be seen. Using all the features of a 256x256 image is impractical and computationally demanding. Firstly, the eigenfaces method reduces the number of features to represent the radiographs, in this case, reducing them to 1000 features. However, the features derived from eigenfaces are ordered according to the variance of the grayscale pixel values. Therefore, the Fisher Ratio (FR) is used as a method to select the features with the highest discriminative power, reducing the number to 600. Finally, the selected features are weighted using the same FR, so that features with greater discriminatory power have a higher impact on classification. This approach creates a reduced and highly efficient set of features for the classification process.

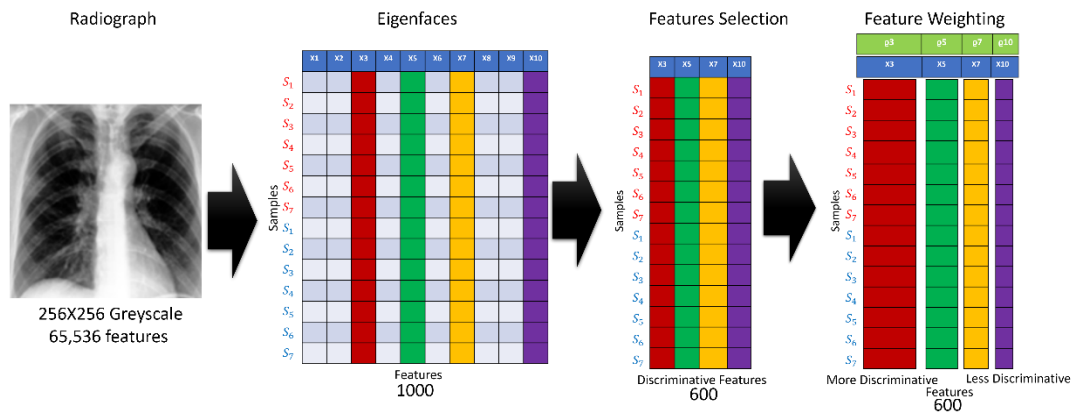


Figure 4. Graphical Representation of the Transformation Applied to the Pixel Gray Values of the Radiographs. Initiating with the Eigenfaces method for dimensional reduction, followed by the FR for feature selection and weighting

#### 4 Image Dataset and Experimental Setup

The image dataset utilized in this study is sourced from the “COVID-19 Radiography Database,” accessible through Kaggle and developed by (Chowdhury et al., 2020; Rahman et al., 2021). This dataset comprises 6,012 images labeled for lung opacity (other lung diseases), viral pneumonia, normal conditions, and COVID-19, with a specific distribution of 6012, 10,192, and 3616 images, respectively. Additionally, the dataset includes masks designed to segment the ROI in the radiographs generated beforehand by Rahman et al. For this study, 1300 **pneumonia** radiographs and 1300 **normal** radiographs were randomly selected, all with a dimension of 256x256 pixels. These images were divided into a training set of 2000 images, evenly distributed with 1000 images for each class. In the testing phase, 600 images were selected, 300 for each class, to ensure a balanced image set.

Figure 5 outlines the procedures applied to the radiographs for conducting the comparative experiments. The objectives are to find the best representation of a radiograph for classification, observe the effect of contrast enhancement on classification, and test whether the proposed feature selection and weighting methodology can compete with CNNs. First, all images undergo semantic segmentation using the masks generated by Rahman, forming a group of segmented images. Simultaneously, the images are normalized using the LFA, forming a group of normalized images. The next image preprocessing step is to apply CLAHE to both groups of images.

The group of classification algorithms includes all architectures available in the MVTEC Deep Learning Tool 23.04 program (MobileNetV2, ResNet-50, ResNet-18, Compact, and AlexNet) and the proposed classifier. For training the CNNs, a batch size of 32, a learning rate of 0.001, and 100 epochs were used. These parameters were chosen because they are compatible with the architecture of all CNNs, and the number of epochs was selected as no improvement was observed with an increase. In the case of the proposed classifier, Eigenfaces were chosen to reduce the dimensionality of the images. Furthermore, the Fisher Ratio (FR) criterion was applied for selecting and weighting the most relevant features based on their discriminatory capacity between classes. Both algorithms were used in conjunction to enhance the discriminative capability of the features before training the MLP. The MLP’s topology was configured with 600 features in the input layer, followed by four hidden layers, each composed of 120 neurons, and a single neuron in the output layer. The MLP training process extended over 100 epochs.

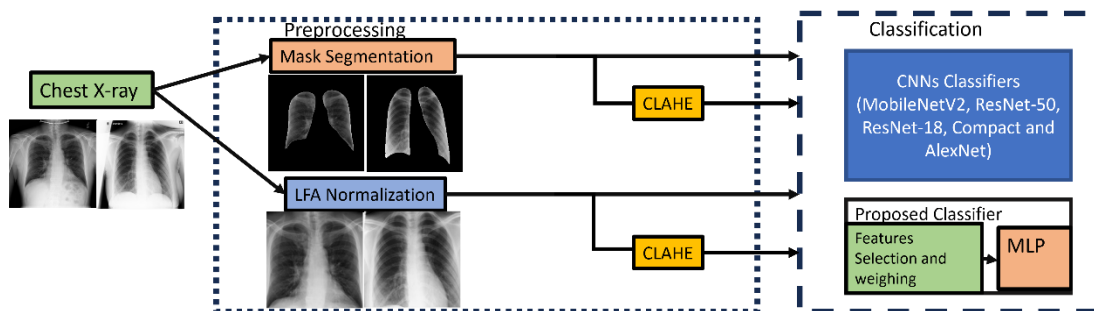


Figure 5. Experiment Sequence In the first experiment, ROI segmentation is performed on the radiographs. In the second experiment, contrast enhancement using CLAHE is added to the segmentation process. In the third experiment, radiographs are normalized using the LFA (Localization and Feature Alignment). In the final experiment, CLAHE is applied to the LFA. Classification is conducted using CNNs and the proposed classifier.

### 5 Results and Discussions

Below in Table 2 are the accuracy results for all the classifier algorithms after applying cross-validation for the comparative experiments.

**Table 2.** Accuracy results of CNNs and the proposed classifier for the experiments

Classifier	Mask Segmentation	LFA Normalization	Mask Segmentation + CLAHE	LFA Normalization + CLAHE
MobileNetV2	<b>95.3%</b>	<b>97.1%</b>	<b>95.3%</b>	<b>97.1%</b>
ResNet-50	91.6%	96%	91.6%	96%
ResNet-18	<b>95.1%</b>	96.3%	<b>95.8%</b>	96.6%
Compact	86.5%	90.8%	86.5%	90.8%
AlexNet	87.5%	90%	86.5%	89.1%
Proposed Classifier	91%	<b>97.3%</b>	91.8%	<b>97.3%</b>

Images generated through ROI segmentation with masks exhibit more significant variability in the shape and size of the lungs compared to those normalized using the LFA. In the first experiment, ResNet-18 and MobileNetV2 stood out as achieving the best results when using segmentation. However, our proposed classifier was negatively affected in this test due to the images' variability, impacting the features generated by the Eigenfaces method. In the second experiment, where images normalized with LFA were employed, our proposed classifier and MobileNetV2 achieved the best performances. Furthermore, all classifiers experienced an increase in accuracy compared to segmented images. This increase is attributed to the lower variability when using normalization with LFA. Our proposed classifier achieves its maximum precision metric when using these normalized images, as it is more compatible with dimensional reduction through Eigenfaces and feature selection and weighting through the Fisher Ratio (FR). This demonstrates that algorithms not based on deep learning can achieve the same or better results.

For the experiments involving contrast enhancement using CLAHE, most CNNs were not significantly affected by the enhancement. ResNet-18 achieved its best results with CLAHE applied, but AlexNet obtained its worst results. These varying outcomes may be due to the different architectures of each CNN. The suggestion for future tests is to compare the classification results on radiographs with and without contrast enhancement, regardless of the classifier algorithm used, to determine if contrast enhancement is appropriate.

In experiments 3 and 4, normalization continued to be the better representation of the radiographs, showing consistency in results, and indicating that normalization is the best representation for radiographs. Additionally, the results in these experiments are competitive with the state-of-the-art, surpassing those obtained with the methodologies proposed by (Budimirovic et al., 2022; Mydhili et al., 2023) for the classification of pneumonia radiographs.

## 6 Conclusions and Future Work

In this study, we introduce an innovative technique for detecting and automatically normalizing the Region of Interest (ROI) in chest radiographs, named LFA (Localization and Feature Alignment). Alongside, we propose a classifier for automatically detecting pneumonia in chest radiographs that leverages feature selection and weighting based on the Fisher Discriminant criterion applied to "Eigenfaces," complemented by a Multilayer Perceptron (MLP) for classification. Through the LFA preprocessing methodology, we achieve an enhanced representation of the radiographs, facilitating their classification using various classifier algorithms, whether based on Convolutional Neural Networks (CNNs) or not.

Furthermore, the results demonstrate that employing ROI alignment as image preprocessing and feature selection significantly increases classification accuracy, especially when using traditional machine learning classifiers like MLP. It is suggested to conduct experiments both with and without contrast enhancement to assess the appropriateness of this technique for the classifier algorithm, as the results obtained in this study exhibit different behaviors. The reliability of the results is supported using cross-validation techniques. Notable contributions of this work include an effective method for ROI normalization in lung images and a technique for selecting highly discriminative features, leveraging the Fisher Discriminant criterion. Our proposal achieves competitive accuracy values compared to state-of-the-art works using CNN-based techniques.

For future research directions, we propose exploring the application of LFA in other sets of lung images to detect different diseases. Additionally, feature selection and weighting could undergo further testing to enhance classification accuracy in other machine-learning algorithms.

## References

1. Alzahrani, S. A., Al-Salamah, M. A., Al-Madani, W. H., & Elbarbary, M. A. (2017). Systematic review and meta-analysis for the use of ultrasound versus radiology in diagnosing of pneumonia. In *Critical Ultrasound Journal* (Vol. 9, Issue 1). <https://doi.org/10.1186/s13089-017-0059-y>
2. Amatya, Y., Rupp, J., Russell, F. M., Saunders, J., Bales, B., & House, D. R. (2018). Diagnostic use of lung ultrasound compared to chest radiograph for suspected pneumonia in a resource-limited setting. *International Journal of Emergency Medicine*, 11(1). <https://doi.org/10.1186/s12245-018-0170-2>
3. Ayala-Raggi, S. E., Picazo-Castillo, A. E., Barreto-Flores, A., & Portillo-Robledo, J. F. (2023). Synergizing Chest X-ray Image Normalization and Discriminative Feature Selection for Efficient and Automatic COVID-19 Recognition. *Lecture Notes in Computer Science (Including Subseries Lecture Notes in Artificial Intelligence and Lecture Notes in Bioinformatics)*, 14407 LNCS. [https://doi.org/10.1007/978-3-031-47637-2\\_17](https://doi.org/10.1007/978-3-031-47637-2_17)
4. Baltazar, L. R., Manzanillo, M. G., Gaudillo, J., Viray, E. D., Domingo, M., Tiangco, B., & Albia, J. (2021). Artificial intelligence on COVID-19 pneumonia detection using chest xray images. *PLoS ONE*, 16(10 October). <https://doi.org/10.1371/journal.pone.0257884>
5. Budimirovic, N., Prabhu, E., Antonijevic, M., Zivkovic, M., Bacanin, N., Strumberger, I., & Venkatachalam, K. (2022). COVID-19 Severity Prediction Using Enhanced Whale with Salp Swarm Feature Classification. *Computers, Materials and Continua*, 72(1). <https://doi.org/10.32604/cmc.2022.023418>
6. Chowdhury, M. E. H., Rahman, T., Khandakar, A., Mazhar, R., Kadir, M. A., Mahbub, Z. Bin, Islam, K. R., Khan, M. S., Iqbal, A., Emadi, N. Al, Reaz, M. B. I., & Islam, M. T. (2020). Can AI Help in Screening Viral and COVID-19 Pneumonia? *IEEE Access*, 8. <https://doi.org/10.1109/ACCESS.2020.3010287>
7. Gazda, M., Plavka, J., Gazda, J., & Drotar, P. (2021). Self-Supervised Deep Convolutional Neural Network for Chest X-Ray Classification. *IEEE Access*, 9. <https://doi.org/10.1109/ACCESS.2021.3125324>
8. Ghaderzadeh, M., Aria, M., & Asadi, F. (2021). X-Ray Equipped with Artificial Intelligence: Changing the COVID-19 Diagnostic Paradigm during the Pandemic. In *BioMed Research International* (Vol. 2021). <https://doi.org/10.1155/2021/9942873>
9. Hamza, A., Attique Khan, M., Wang, S. H., Alhaison, M., Alharbi, M., Hussein, H. S., Alshazly, H., Kim, Y. J., & Cha, J. (2022). COVID-19 classification using chest X-ray images based on fusion-assisted deep Bayesian



- optimization and Grad-CAM visualization. *Frontiers in Public Health*, 10. <https://doi.org/10.3389/fpubh.2022.1046296>
10. Kavitha, M., Srinivsan, R., Triveni, K., & Chowdary, C. P. (2023). Pneumonia Detection Using Deep Learning Techniques. *2023 IEEE International Conference on Research Methodologies in Knowledge Management, Artificial Intelligence and Telecommunication Engineering, RMKMATE 2023*. <https://doi.org/10.1109/RMKMATE59243.2023.10369493>
  11. Khan, A., Khan, S. H., Saif, M., Batool, A., Sohail, A., & Waleed Khan, M. (2023). A Survey of Deep Learning Techniques for the Analysis of COVID-19 and their usability for Detecting Omicron. *Journal of Experimental and Theoretical Artificial Intelligence*. <https://doi.org/10.1080/0952813X.2023.2165724>
  12. Kirby, M., & Sirovich, L. (1990). Application of the Karhunen-Loève Procedure for the Characterization of Human Faces. *IEEE Transactions on Pattern Analysis and Machine Intelligence*, 12(1). <https://doi.org/10.1109/34.41390>
  13. Kundur, N. C., Anil, B. C., Dhulavvagol, P. M., Ganiger, R., & Ramadoss, B. (2023). Pneumonia Detection in Chest X-Rays using Transfer Learning and TPUs. *Engineering, Technology and Applied Science Research*, 13(5), 11878–11883. <https://doi.org/10.48084/ETASR.6335>
  14. Lee, H., Choo, H., Le, D. T., & Bum, J. (2023). Chest Radiographs Enhancement with Contrast Limited Adaptive Histogram. *Proceedings of the 2023 17th International Conference on Ubiquitous Information Management and Communication, IMCOM 2023*. <https://doi.org/10.1109/IMCOM56909.2023.10035649>
  15. Moberg, A. B., Taléus, U., Garvin, P., Fransson, S. G., & Falk, M. (2016). Community-acquired pneumonia in primary care: Clinical assessment and the usability of chest radiography. *Scandinavian Journal of Primary Health Care*, 34(1). <https://doi.org/10.3109/02813432.2015.1132889>
  16. Mohammed, B. N., Al-Mukhtar, F. H., Yousif, R. Z., & Almashhadani, Y. S. (2021). Automatic Classification of Covid-19 Chest X-Ray Images Using Local Binary Pattern and Binary Particle Swarm Optimization for Feature Selection. *Cihan University-Erbil Scientific Journal*, 5(2), 46–51. <https://doi.org/10.24086/CUESJ.V5N2Y2021.PP46-51>
  17. Mydhili, S. K., Venkatesh, C., Amrin, Z., & Jaya Dharani, M. (2023). CNN based Deep Learning for Pneumonia Detection. *12th IEEE International Conference on Advanced Computing, ICoAC 2023*. <https://doi.org/10.1109/ICOAC59537.2023.10249251>
  18. Niederman, M. S., & Torres, A. (2022). Severe community-acquired pneumonia. *European Respiratory Review*, 31(166). <https://doi.org/10.1183/16000617.0123-2022>
  19. Nillmani, Sharma, N., Saba, L., Khanna, N. N., Kalra, M. K., Fouda, M. M., & Suri, J. S. (2022). Segmentation-Based Classification Deep Learning Model Embedded with Explainable AI for COVID-19 Detection in Chest X-ray Scans. *Diagnostics*, 12(9). <https://doi.org/10.3390/diagnostics12092132>
  20. Qin, C., Yao, D., Shi, Y., & Song, Z. (2018). Computer-aided detection in chest radiography based on artificial intelligence: A survey. In *BioMedical Engineering Online* (Vol. 17, Issue 1). <https://doi.org/10.1186/s12938-018-0544-y>
  21. Rahman, T., Khandakar, A., Qiblawey, Y., Tahir, A., Kiranyaz, S., Abul Kashem, S. Bin, Islam, M. T., Al Maadeed, S., Zughaier, S. M., Khan, M. S., & Chowdhury, M. E. H. (2021). Exploring the effect of image enhancement techniques on COVID-19 detection using chest X-ray images. *Computers in Biology and Medicine*, 132. <https://doi.org/10.1016/j.compbiomed.2021.104319>
  22. Ramli, A. A. B., Zulkifli, Z., Ahmad, S., & Ghazali, N. (2023). Automatic Pneumonia Detection Through Chest X-Ray Image-Based. *2023 4th International Conference on Artificial Intelligence and Data Sciences: Discovering Technological Advancement in Artificial Intelligence and Data Science, AiDAS 2023 - Proceedings*, 355–360. <https://doi.org/10.1109/AIDAS60501.2023.10284669>
  23. Salvatore, C., Interlenghi, M., Monti, C. B., Ippolito, D., Capra, D., Cozzi, A., Schiaffino, S., Polidori, A., Gandola, D., Ali, M., Castiglioni, I., Messa, C., & Sardanelli, F. (2021). Artificial intelligence applied to chest x-ray for differential diagnosis of covid-19 pneumonia. *Diagnostics*, 11(3). <https://doi.org/10.3390/diagnostics11030530>
  24. Silva, T. S. (2019a). An illustrative introduction to Fisher's Linear Discriminant. <https://Sthalles.Github.io>. <https://sthalles.github.io/fisher-linear-discriminant/>
  25. Silva, T. S. (2019b). An illustrative introduction to fisher's linear discriminant. <https://Sthalles.Github.io/Fisher-Linear-Discriminant/>.
  26. Ticinesi, A., Lauretani, F., Nouvenne, A., Mori, G., Chiussi, G., Maggio, M., & Meschi, T. (2016). Lung ultrasound and chest x-ray for detecting pneumonia in an acute geriatric ward. *Medicine (United States)*, 95(27). <https://doi.org/10.1097/MD.00000000000004153>
  27. Turk, M. A., & Pentland, A. P. (1991). Face recognition using eigenfaces. *Proceedings. 1991 IEEE Computer Society Conference on Computer Vision and Pattern Recognition*, 586–591. <https://doi.org/10.1109/CVPR.1991.139758>
  28. Turk, M., & Pentland, A. (1991). Eigenfaces for recognition. *Journal of Cognitive Neuroscience*, 3(1). <https://doi.org/10.1162/jocn.1991.3.1.71>
  29. World Health Organization. (2016). WHO | Pneumonia. In *Who*.